INL/JOU-24-76262-Revision-0

Design of a first-of-A-kind instrumented advanced test reactor irradiation Capsule experiment for In situ thermal conductivity measurements of metallic fuel

Changing the World's Energy Future

Nate Oldham, Angelica Mata Cruz, Calvin Myer Downey, Daniel B Chapman, Kelly D Ellis, Austin D Fleming

Idaho National Laboratory

INL/JOU-24-76262-Revision-0

Design of a first-of-A-kind instrumented advanced test reactor irradiation Capsule experiment for In situ thermal conductivity measurements of metallic fuel

Nate Oldham, Angelica Mata Cruz, Calvin Myer Downey, Daniel B Chapman, Kelly D Ellis, Austin D Fleming

October 2024

Idaho National Laboratory
Idaho Falls, Idaho 83415

http://www.inl.gov

Prepared for the
U.S. Department of Energy
Under DOE Idaho Operations Office
Contract DE-AC07-05ID14517

Design of a First-Of-A-Kind Instrumented Advanced Test Reactor Irradiation Capsule Experiment for In Situ Thermal Conductivity Measurements of Metallic Fuel

[1]Calvin M. Downey, [1]Nathaniel Oldham, [2]Austin Fleming, [3]Daniel Chapman, [4]Angelica Mata Cruz, [5]Kelly Ellis

[1]Experiment Design Department, Idaho National Laboratory, Idaho Falls, ID 83415
[2]Measurement Sciences, Idaho National Laboratory, Idaho Falls, ID 83415
[3]Experiment Thermal Hydraulics Analysis Department, Idaho National Laboratory, Idaho Falls, ID 83415
[4]Neutronics Analysis Department, Idaho National Laboratory, Idaho Falls, ID 83415
[5]Engineering Structural Analysis Department, Idaho National Laboratory, Idaho Falls, ID 83415

ABSTRACT

Metallic fuel undergoes dramatic microstructural changes early in life due to fission gas swelling until ~2–3 at% burnup which affects the conductivity of the material, however the evolution of metallic fuel thermal conductivity during this early phase burnup has never been successfully measured in situ. The Irradiated Material Properties Accelerated Characterization Test (IMPACT) experiment will be the first in a series of experiments to irradiate advanced nuclear metallic fuel specimens with novel embedded thermal conductivity probes in ATR. In the current work the IMPACT experiment final design and supporting analysis is reported in detail. Results are evaluated for various reactor operational conditions to meet the functional requirements of the experiment. The first iteration of this IMPACT experiment will provide data regarding thermal properties evolution in uranium-zirconium (U10Zr) fuel, but this experiment vehicle is envisioned for future advanced fuels and structural materials irradiations in ATR.

Keywords: Nuclear experiment design, metallic fuel, thermal conductivity, instrumentation

1. INTRODUCTION

In situ measurements in irradiation environments are challenging because of the harsh irradiation conditions as well as significant engineering required to facilitate data transmission lines to and from the reactor core. Idaho National Laboratory (INL) is developing a first-of-a-kind instrumented capsule experiment designed to enable in situ measurement capabilities in the Advanced Test Reactor (ATR) core. This capability will provide direct access to parameters more commonly inferred through post-irradiation measurements and modeling, and minimize specimen throughput (by reducing physical testing quantities) by extracting more specimen information during irradiation testing. Utilizing the recent installation of the ATR Top Head Closure Plate–Mark II (THCP-MkII), penetrations out of ATR have been increased to allow for instrumented capsules from both I-positions and Small-B positions, effectively doubling the experiment penetration capacity through the top of ATR. The Irradiated Material Properties Accelerated Characterization Test (IMPACT) experiment will be the first in a series of experiments to irradiate various advanced nuclear fuel specimens and materials with embedded thermal conductivity probes in ATR.

The Department of Energy's Office of Nuclear Energy (DOE-NE) oversees research and development of advanced fast-spectrum nuclear fuel technologies, especially metallic fuels intended for Sodium Fast Reactors (SFR), by filling data gaps not addressed in past research. IMPACT, the first iteration of this experiment, will generate data describing the thermal properties evolution of three metallic fuel designs to help mature fuel performance models and optimize reactor designs using uranium 10 weight percent (wt%) zirconium (U10Zr) fuel and will demonstrate a new method for accelerated characterization of nuclear fuel properties. Metallic fuel alloys have long been under investigation for use in advanced reactors due to their high thermal conductivity. During irradiation, metallic fuel undergoes dramatic microstructural changes early in life due to fission gas swelling until ~2–3 atomic percent (at%) burnup when pores interconnect, thus allowing fission gas to escape into the fuel pin plenum and swelling effectively ceases. The U10Zr fuel system is an ideal candidate for this experiment due to its currently high and growing commercial interest as a high density, good thermal performance fuel, making it ideal for many applications including compact high power density reactor designs. However, the evolution of metallic fuel thermal conductivity during this early phase burnup (and over the course of burnup) has never been successfully measured in situ in-pile [1]. Post-irradiation examination (PIE) measurements made by Bauer gave a measurement uncertainty of ±20% for nine discrete local burnup values (ranging between 0.5–1.9 at% burnup). The embedded conductivity probe capability allows for continuous measurements rather than discrete points, and previous laboratory testing has demonstrated the technique is capable of thermal property measurement with uncertainty better than 10% on a range of sample materials. Therefore, more accurate measurements that utilize advanced thermal conductivity probes have the potential to significantly improve the understanding of this fuel system's behavior. In the current work, the IMPACT experiment final design and supporting analysis is detailed, and results are evaluated for various reactor operational conditions to meet the functional requirements of the experiment.

2. DESIGN OVERVIEW AND FUNCTIONAL REQUIREMENTS

The IMPACT experiment is designed to irradiate three different designs of metallic fuel in ATR and considers both programmatic and operational requirements. The three variations of fuel specimens are: sodium-bonded annular fuel specimen, non-bonded annular fuel specimen, and a grooved annular fuel specimen, as shown in Figure 1a. Fuel specimen requirements are summarized in Table 1. Each fuel specimen in the experiment accommodates a thermal conductivity needle probe in the axial centerline of the fuel which will record thermal conductivity of the fuel in situ. This sensor was developed by INL's Measurement Sciences Laboratory (MSL). The sodium-bonded specimen will consist of a loose-fitting fuel section with a central hole, and with a sodium thermal bond inside of the cladding designed to prevent sodium from contacting the probe surface. The non-bonded specimen consists of a tight-fitting fuel section with a central hole for the probe. The grooved annular specimen consists of a tight-fitting fuel section with three hemispherical grooves (120 degrees apart) along the length of the specimen. In the experiment assembly an SS316L baseline capsule is used to provide a thermal conductivity reference point during irradiation. Because the temperature-dependent thermal conductivity of stainless steel (SST) is well documented, the reference conductivity of the baseline can give supplemental information on signal drift due to irradiation in the core.

Each fuel design is sealed into a rodlet with a cladding inner diameter (ID) of 4.95 mm with sufficient plenum space to contain fission gas produced during irradiation. This rodlet is separated from the primary coolant system (PCS) by multiple capsule containments as shown in Figure 1b. The outer capsule is considered the primary pressure boundary which separates the dry interior experiment from the reactor PCS. The experiment outer capsule boundary is assembled in a way that allows shared gas communication between the internal volume of the outer capsules, forming what is colloquially known as the in-core test train. An instrument leadout tube is designed connect the in-core test train portion of the experiment to an I-position penetration through the ATR top head closure plate (THCP). These critical design requirements are discussed in detail in later sections. The outer capsule boundary and leadout components act as the primary pressure boundary and were designed, fabricated, and inspected to ASME BPVC Section III, Class 3 [2]. Hardware sealing the experiment through the THCP penetration is designed, fabricated, and inspected to ASME BPVC Section III, Class 1 [3]. Additional requirements involving specimen temperatures and power, the structural integrity of the experiment during operation, and neutronics impacts are discussed in this section.

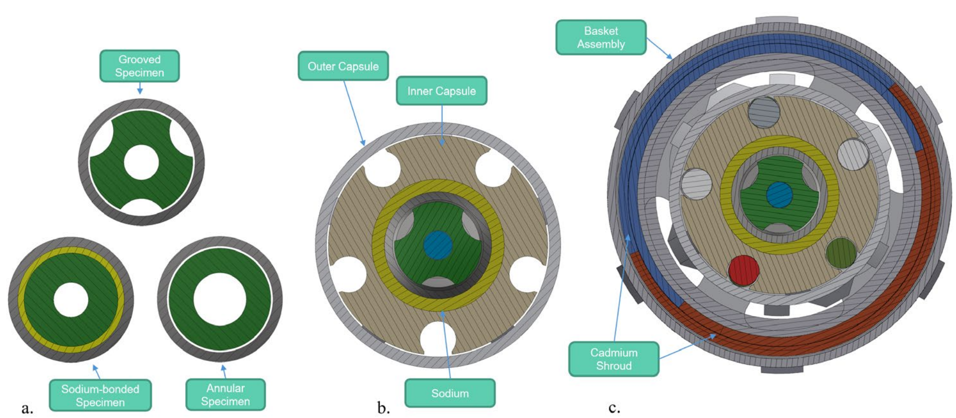

Figure 1: Shows cross-section views of a.) fuel rodlets, b.) inner and outer capsules, and c.) installation of experiment in a cadmium shrouded basket.

Table 1: Shows key functional requirements of the irradiation experiment.

Figure	Characteristic	Value
Fuel Form	Target	U10Zr
Burnup	Minimum	2.5% per cycle
Smear Density	Target	75%
Fuel-cladding Temperature	Target	500–650°C
Power Density	Target	325±50 W/cm
Radial Power Peaking	Target	1.5× average
Plenum Gas	N/A	Helium

The IMPACT experiment will irradiate the three metallic fuel specimens within a cadmium shrouded basket as shown in Figure 1c in an ATR small-B position on the east side of the reactor, otherwise described as the east lobe as pictured in Figure 2. Specifically, the IMAPCT experiment targets insertion into the eastern B3 position. Cadmium shrouded baskets have historically been used in ATR experiments to filter out the thermal neutron spectrum in the experiment to achieve more prototypic neutron irradiation conditions for fuels intended for use in fast-spectrum cores. In other words, cadmium baskets will reduce the total fluence on an experiment by absorbing thermal neutrons, but the spectrum achieved is predominantly fast spectrum (considered broadly to be >0.1MeV). Cadmium-shrouded baskets were designed for interfacing with ATR small-B positions.

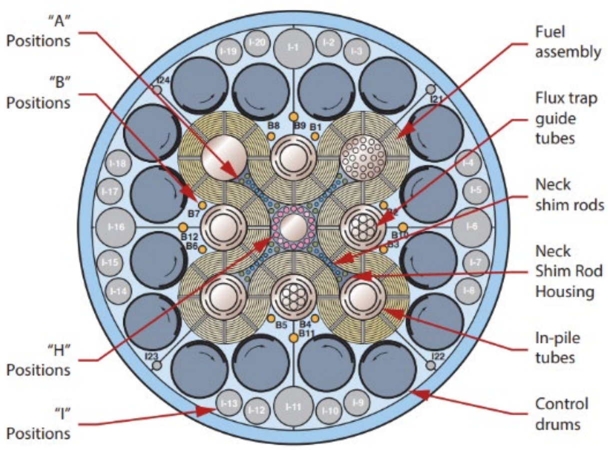

Figure 1: Shows a cross section of the ATR core with various irradiation positions and assemblies labeled.

Neutronics analysis on the fuel is initially performed for fuel enrichment scoping to reach the desired linear heat generation rate (LHGR) in the core and to determine any potential radial power peaking in the fuel specimens. LHGRs were used in thermal hydraulic analysis to ensure the desired fuel-cladding temperatures in the experiment. Temperatures in the experiment were designed with a one-time tuning of the size and mixture of an inert gas gap between the inner and outer capsule. Normal operation of these experiments is described under Service Level A per ASME BPVC Section III [2], [3]. During irradiation and normal operating conditions, the pressure in the outer capsule containment must not reach over 1.62 MPa to meet ASME BPVC Section III, Class 3 [2] designation (rather than Class 1 [3]) per the ATR safety analysis report (SAR). Experiment temperature shifts due to the off-normal ASME BPVC Section III Service Level C [2], [3] events due to flow coastdown or reaction insertion accident (RIA) and a Service Level D [2], [3] conditions were also considered in further structural analysis for outer capsules. ASME BPVC Section III Service Level D events are considered singular unlikely probability events. The experiment outer boundaries must survive all possible operating conditions considered in the design. Experiment hardware sealing through the THCP-MkII must also be shown to service ASME BPVC Section III Service Levels A and C operating conditions.

3. Mechanical Design

3.1 Instrumentation and Data Acquisition

The experiment thermal conductivity probe uses a frequency-domain-based measurement system to provide a reliable in situ measurement of temperature and thermal conductivity. This method has never before been used in-reactor, and it is applicable to a variety of advanced fuel forms and materials. The underlying theory of the frequency domain probe was recently developed at INL [4], [5]. The thermocouple depicted as green in Figure 3 provides a centerline temperature measurement, while the heater wire depicted as blue in Figure 2 acts as a periodic heat source. The lock-in amplifiers provide accurate measurements of the amplitude and phase of the temperature compared to periodic heating. The lock-in amplifiers act as an adjustable, narrow bandpass filter, which enables accurate measurements when the noise may be several orders of magnitude larger, which is a great advantage for electrically noisy environments such as reactors. The probe uses a four-wire design which eliminates the impact of long lead lengths on the measurement by separating the current supply and voltage taps, depicted as red and orange in Figure 2. This is important for in-pile applications where lead lengths can be on the order of 20 meters. Additionally, the technique only requires the phase between temperature and heating to extract the thermal properties, so sensor drift does not necessarily impact the measurement since an absolute temperature measurement is not required. The custom probe is fabricated at INL using standard mineral-insulated cable manufacturing techniques, like those used in the fabrication of high-temperature thermocouples.

The technology provides several strategic advantages by simultaneously measuring the temperature and thermal properties of the fuel system. Under this project, the probe will need to be optimized to explore the targeted metallic fuel system in the first in-pile demonstration of this sensor. Four thermal conductivity probes and two thermocouples (TCs) (one single-point and one multipoint) will provide in situ data during the IMPACT experiment. Mineral-insulated cabling (MIC) from the thermal conductivity sensor and TCs are transitioned to high-temperature fiberglass cables in the leadout section of the experiment above the reactor core. Cabling will be sealed out through the top of the experiment via a custom epoxy hermetic seal to ensure the helium gas gap atmosphere is maintained in the outer capsule. Existing conduit lines connect experiment connectors outside of the reactor and route signal output to the data acquisition system (DAS).

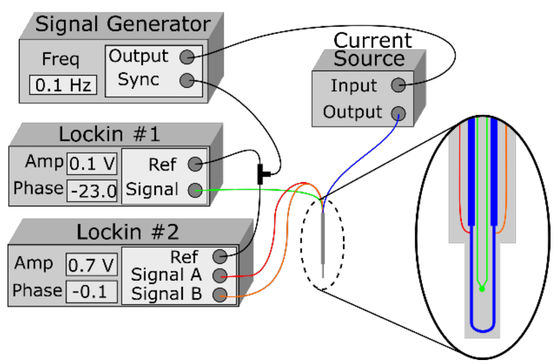

Figure 2: Shows a schematic of the thermal conductivity probe and signal processing.

3.2 Integration into Existing Reactor Interfaces

The IMPACT experiment is slated for insertion into the ATR B3 small-B position. The experiment is lifted into position via an overhead crane and inserted through the slated I-penetration in ATR THCP-MkII. Prior to the experiment installation, the cadmium-shrouded experiment basket and spring-loaded test stop are installed into the B3 position. The spring-loaded test stop assembly sits in the bottom of the cadmium-shrouded-basket to add support during installation and to act as a spacer to locate specimens at the desired axial location in the core. Once the experiment is installed into the position, it is bottom-weighted into the cadmium-shrouded basket; however, after the experiment is sealed through the ATR THCP-MkII, it will hang from the THCP-MkII in the position. Standard ATR hook tooling will interface with handling rings on the outside of the leadout portion of the experiment boundary, which will assist with operator installation and eventual removal of the experiment after irradiation. Because the THCP-MkII I-penetration and the small-B3 position are not coaxially aligned, an offset jog is required in the leadout section of the experiment 9.58 cm over 1.52 m to reach the reactor

THCP-MkII exit. To both support the experiment during ATR operation and reduce concerns of flow-induced vibration (from horizonal flow in this leadout section), a lateral support arm (LSA) is utilized to connect the leadout section to T-bar supports on the inner wall of the ATR vessel and interfaces with the experiment via a welded support collar. The installation of the IMPACT experiment is shown in Figure 4. All leadout components are fabricated from SS316L pipe and round bar and used by hand-tungsten-inert-gas (TIG) welding qualified to ASME Section IX for final assembly. The leadout components are assembled to the in-core test train portion of the experiment with a reducing transition component between the larger diameter pipes 3.81 cm and the smaller test-train outer capsule diameter of 12.36 mm). Where this transition occurs, there is a potting cup transition from the sensor MIC to the high-temperature fiberglass cables. Below this cable transition, between the leadout and the in-core test train is a fluted tungsten shine path shield which absorbs any radiation that may shine from the in-core experiment into the leadout (gamma irradiation may damage soft cabling and pose risks for operations).

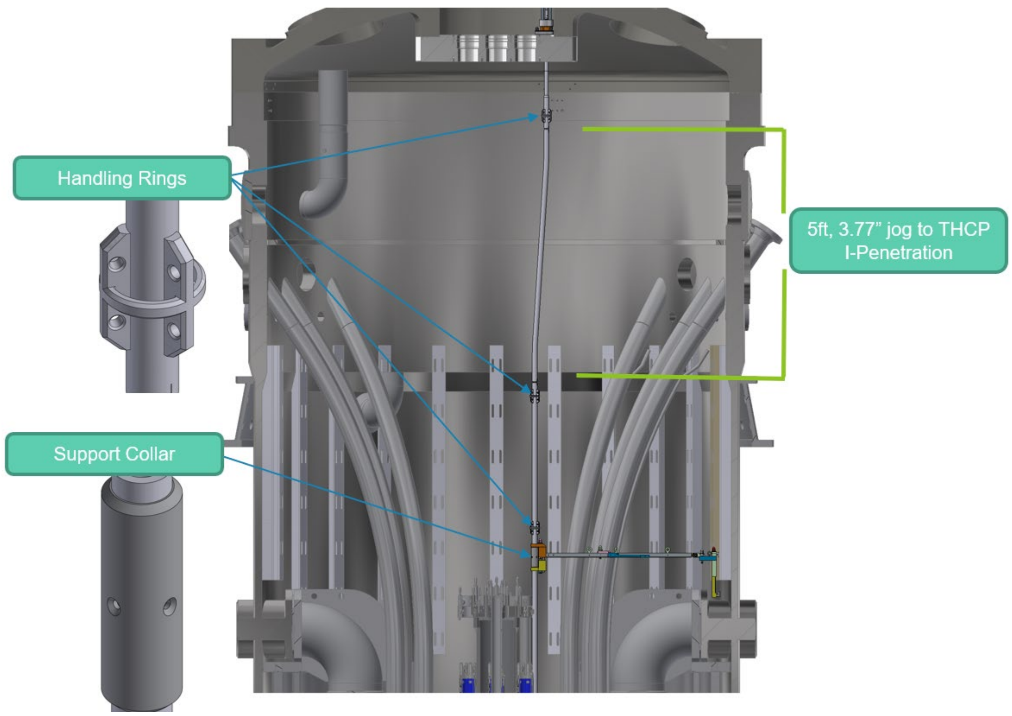

Figure 3: A break-out view of the IMPACT experiment leadout section installed in ATR. THCP-MkII seal hardware seals the experiment through the top of the reactor, handling rings are used for installation, and the support collar interfaces with the LSA.

At the THCP-MkII interface, the experiment will seal to the existing geometry of the THCP-MkII I-Penetration. A seal plug seals the inner surface of the penetration via three O-rings and is held down to the THCP-MkII with the THCP-MkII seal flange (bolted in three places to existing studs on the reactor top head). A washer on the top of the seal flange keys into locations on the seal plug to prevent rotation. The seal sleeve seals the surface between the experiment leadout outer diameter and the inner surface of the seal plug, as well as the surface between the seal plug and the seal sleeve with three O-rings on either surface. This seal sleeve is held down by the seal ring, which is threaded onto ACME-2G threads on the external surface of the experiment leadout, and the seal ring is prevented from unthreading via fasteners into the seal plug. The completed installation of THCP-MkII hardware is pictured in Figure 5. All threaded components and fasteners used in the seal hardware are fabricated from Nitronic 60 SST to prevent thread galling from repeated installation and removal. All components associated with sealing the experiment through the ATR THCP-MkII are fabricated to ASME BPVC Section III Class 1 requirements [3]. Above the sealing hardware, an experiment-extension mast increases the height of the experiment above the THCP-MkII for operator ease-of-access to connectors and hardware. This is further extended toward the maximum height allowable inside of what is known as a shield cylinder, which is the covered section of the ATR

THCP-MkII by the transfer shield plate (TSP). This extension is historically used to prevent any possible release of the seal plug (due to mechanical failure of the sealing hardware) by interfering with the heavy TSP above. Existing cabling connects to the experiment connectors and is routed from the ATR donut through facility conduit to the DAS.

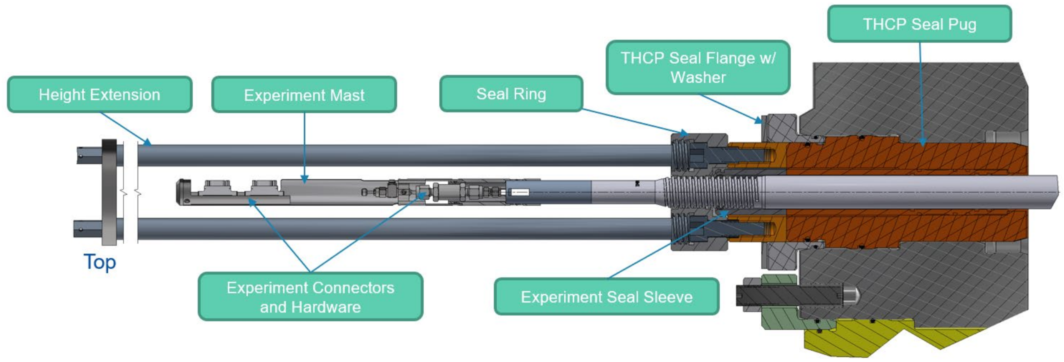

Figure 4: A cross-section view of the IMPACT experiment sealing hardware installed onto the reactor THCP-MkII.

3.3 Capsule In-Core Test-Train Design

The design of the IMPACT rodlet is novel because of its use of an integral capsule bulkhead, which both the inner capsule and outer capsule connect to. The capsule bulkhead acts as part of the ASME BPVC Section III, Class 3 boundary [2]. Standoff nubs on the capsule bulkhead were designed to interface with the inner diameter of the cadmium-shrouded basket. The rodlet components and capsule bulkhead are SS316L. Each thermal conductivity sensor is sealed through the capsule bulkhead with a nickel-based high-temperature braze procedure qualified to ASME Section IX. An autogenous TIG weld qualified to ASME Section IX [6] attaches the rodlet endplug to the rodlet tube, and the rodlet tube to the capsule bulkhead. The autogenous TIG welds are performed under a glovebox with pure helium atmosphere to ensure a helium fill inside of the specimen rodlets. The design of the annular and slotted fuel specimen rodlet is shown in Figure 6.

For the sodium-bonded specimen shown in Figure 7, the fuel and a splash guard are sodium bonded to the rodlet tube. The sodium splash guard is designed to prevent melted sodium operation from expanding and wicking up the rodlet walls, leaking into the fuel central hole, and creating an interference between the thermal conductivity sensor and the fuel. Due to the high thermal conductivity of sodium, the buffer layer of sodium would negatively affect the conductivity measurements of the fuel system during irradiation. This splash guard is threaded into the top of the fuel specimen and creates surface-to-surface contact in the threaded joint to prevent sodium leakage. To ensure continued wall-to-wall contact and seal, it is critical to account for thermal expansion coefficients between the fuel specimen and the splash guard; therefore, depleted U10Zr was the chosen material for the splash guard. Neutronic analysis of the sodium-bonded specimen capsule revealed that the heating rate of the depleted uranium during operation results in undesirable temperatures surrounding the thermal conductivity prob, particularly in the plenum region uncovered by the sodium buffer. Therefore, the splash guard requires a conductive path toe the rodlet cladding and a wave conductor component was designed to ensure surface contact and conduction out of the splash guard to the cladding.

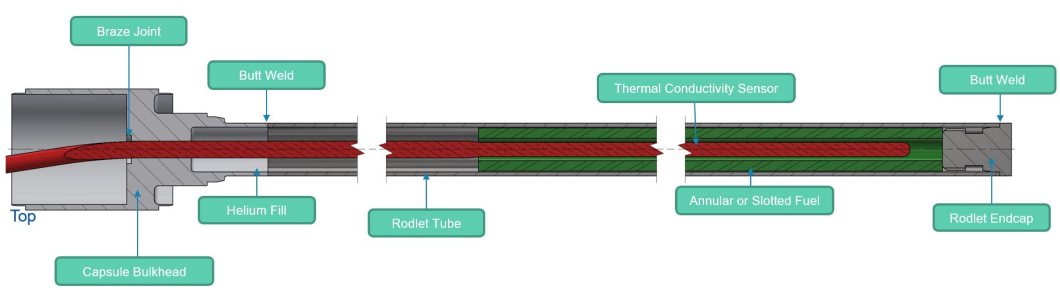

Figure 5: Shows a cross-section view of the IMPACT rodlet assembly.

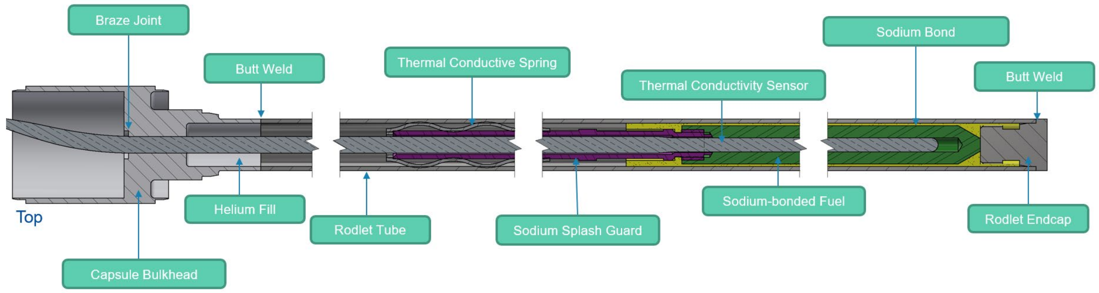

Figure 6: Shows a cross-section view of the IMPACT sodium-bonded rodlet assembly.

The inner capsule components are all S316L with specified low-sulfur content. Inner capsules are designed with hemispherical slots along the length to allow sensors from capsules lower in the test train to route around capsules higher in the test train. Both the single-point TC and the multipoint TC are shown in Figure 8, attached to the sodium-bonded inner-capsule assembly. Dummy instruments in empty slots around the inner capsule create uniform radial heat transfer around the inner capsule, outer diameter, as shown in Figure 13, below, in Section 5. Laser-etched markings on the inner capsule identify the instrument designations for each inner-capsule slot, and laser-etched alignment marks on the bulkhead ensure capsule slot alignments over the length of the capsule test train. Materials are specified to ASME BPVC Section III, Class 3 [2]. An autogenous TIG weld attaches the inner-capsule end cap to the inner-capsule tube, as shown in Figure 8. The inner capsule is sodium bonded over the rodlet assembly and welded to the capsule bulkhead with an autogenous TIG weld. Typically, double-encapsulated, fueled ATR experiments employ a sodium bond between the outer diameter of the rodlet and the inner capsule to smear out any eccentricities in axial and radial conduction, which can occur due to machining tolerances or warping due to welding, as well as the axial position of the fuel specimens within the core. Both autogenous TIG welds are qualified to ASME BPVC Section IX [6] and performed in a glovebox under an inert helium atmosphere.

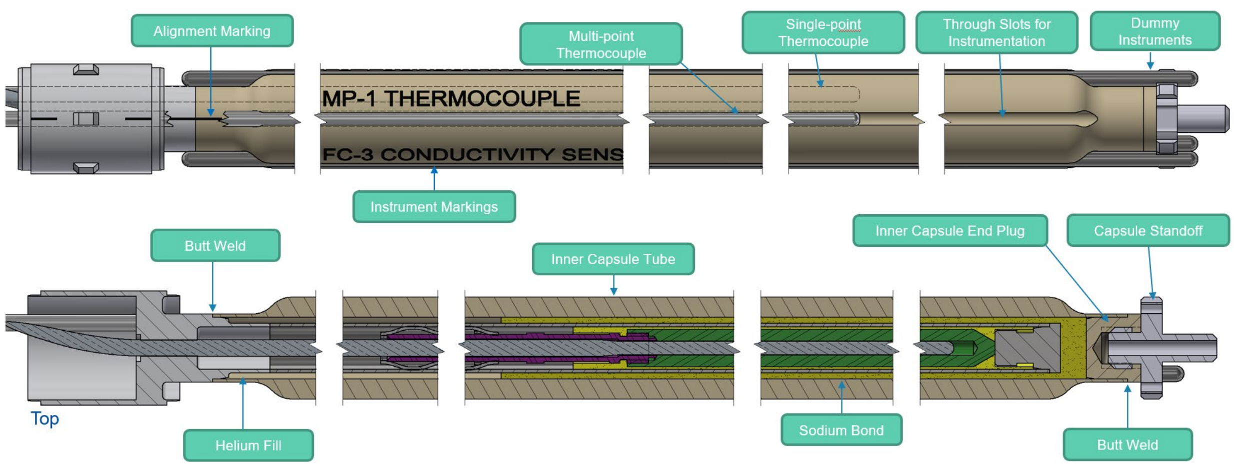

Figure 7: Shows a cross-section view of the IMPACT inner-capsule assembly (with the sodium-bonded rodlet shown).

Outer capsules assemblies are shown in Figure 9 and Figure 10. The outer capsule boundary is fabricated from SS316L, specified with low-sulfur content and to ASME BPVC Section III, Class 3 [2]. The capsule standoff component seen in Figure 8 through 10 is machined from aluminum 6061-T6 series (Al6061-T6), precision ground to the inner diameter of the outer capsule, and threaded into the inner-capsule end plug. This component is designed for field fitment during assembly and precision match machining is required to achieve a 0.10 mm nominal gas gap at beginning of irradiation (BOI) between the inner-capsule outer diameter and the outer-capsule inner diameter for each capsule. Once the standoff fitment is satisfactory, it is held permanently in place with thread sealant. The SST baseline capsule, shown in Figure 10, features only an SST slug with a center-drilled hole for the thermal conductivity sensor. This slug is welded to the capsule bulkhead with the same weld procedure specification as with the inner capsules in the assembly; however, this will not create a sealed environment, and does not need to meet the intent of ASME BPVC Section III, Class 3 [2]. The same Al6061-T6 standoff component maintains a 0.10mm nominal gas gap for the SST baseline capsule.

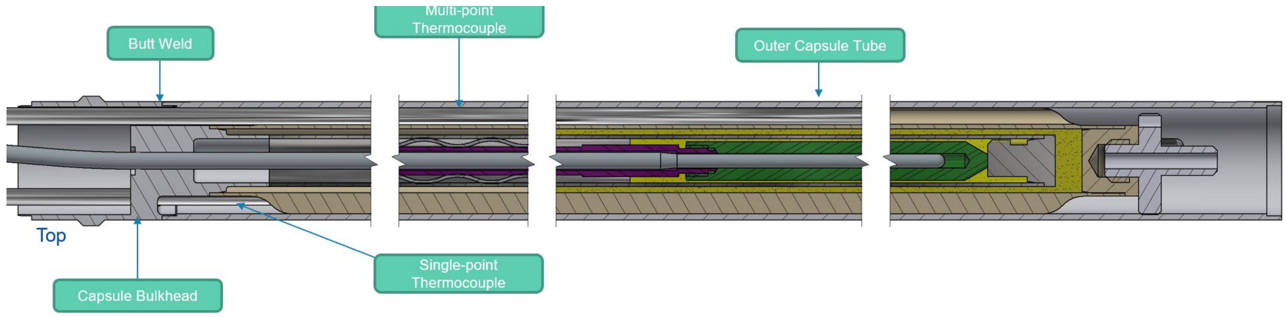

Figure 8: Shows a cross-section view of the IMPACT outer capsule assembly.

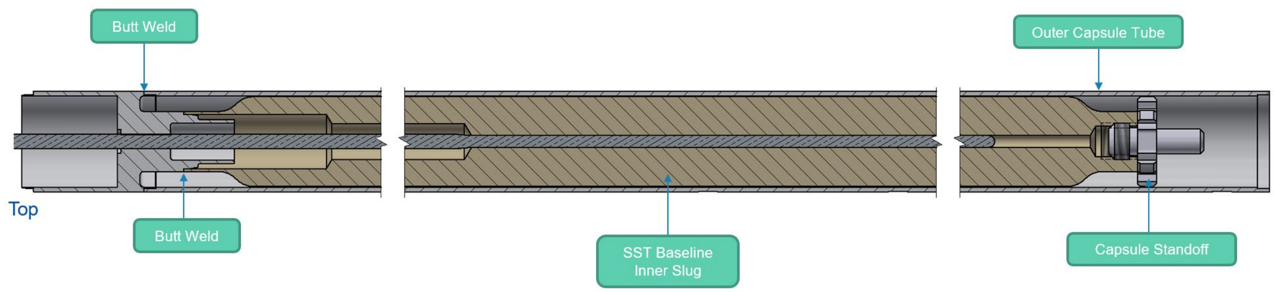

Figure 9: Shows a cross-section view of the IMPACT SST baseline outer capsule assembly.

The capsules are welded together in the desired test-train order, as shown in Figure 11. Laser-etched capsule numbers and nomenclature identify each capsule fuel specimen and location in the test train. As shown in Figure 10, the test train order from bottom to top is the sodium-bonded specimen capsule, annular fuel specimen capsule, annular slotted fuel specimen capsule, and SST baseline capsule. Alignment marks previously laser etched on the capsule bulkhead aligns instrument routing during the capsule test train assembly. Cut marks are etched and located between each capsule for eventual separation and analysis in PIE. The capsule test train is attached to the leadout portion and a 1.21 MPa helium atmosphere is backfilled into the capsule in-core test train via a valve at the top of the experiment assembly.

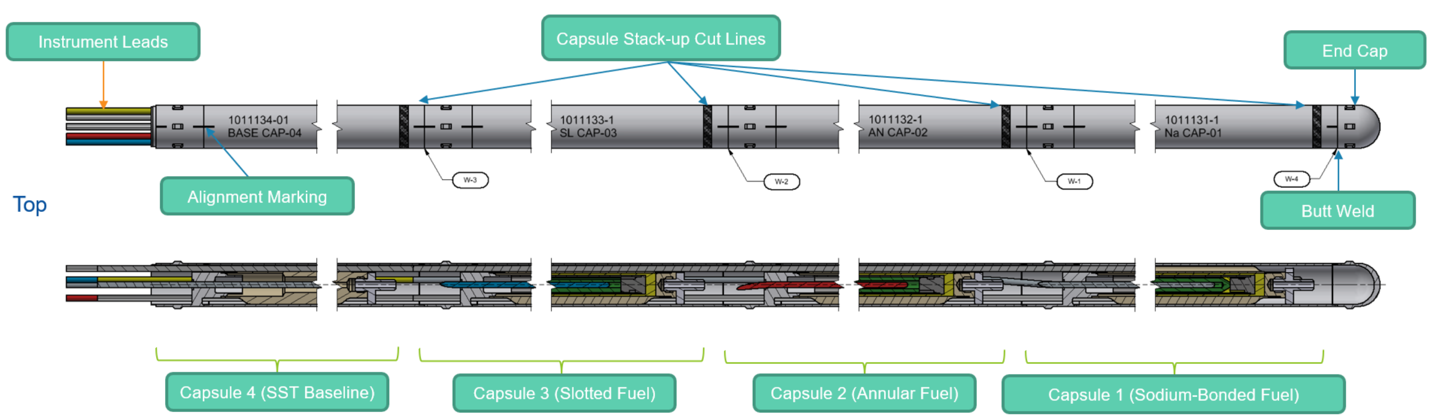

Figure 10: Shows a cross-section view of the IMPACT in-core test train assembly.

4. DESIGN ANALYSIS

4.1 NEUTRONIC ANALYSIS

Neutronic analysis was performed on the IMPACT in-core capsule test train to calculate neutron and gamma heating for fuel and experiment components, radial power in each fuel system, fuel specimen burnup, and moles of fission gas produced. Iterations of neutronics analysis directly informed aspects of mechanical design to meet the requirements of the experiment as they informed fuel LHGRs and burnup, cladding temperatures, temperatures in boundaries, and pressures due to fission gas release. The IMPACT in-core capsule test train was modeled and evaluated in the general-purpose Monte Carlo N-Particle (MCNP 6.2) transport code. The COUPLE and ORIGEN modules of SCALE 6.2.4 were used to deplete fuel specimens and the cadmium basket shrouds, provide time-dependent isotopics, and calculate decay heats in the experiment. The MCNP ORIGEN Activation Automation (MOAA) was used as a tool to automatically pass and couple MCNP results into ORIGEN. In-cell cards were modeled to the dimensions of the computer-aided design (CAD) drawings provided by mechanical design. The experiment was modeled in the ATR core, where the center midplane of the annular specimen is aligned with the ATR core midplane via the test stop spacer at the bottom of the cadmium basket. Each fuel specimen was modeled in four distinct sections to provide information on axial power distributions in the fuel specimen. An example of the MCNP model of the annular slotted specimen capsule is shown in Figure 12.

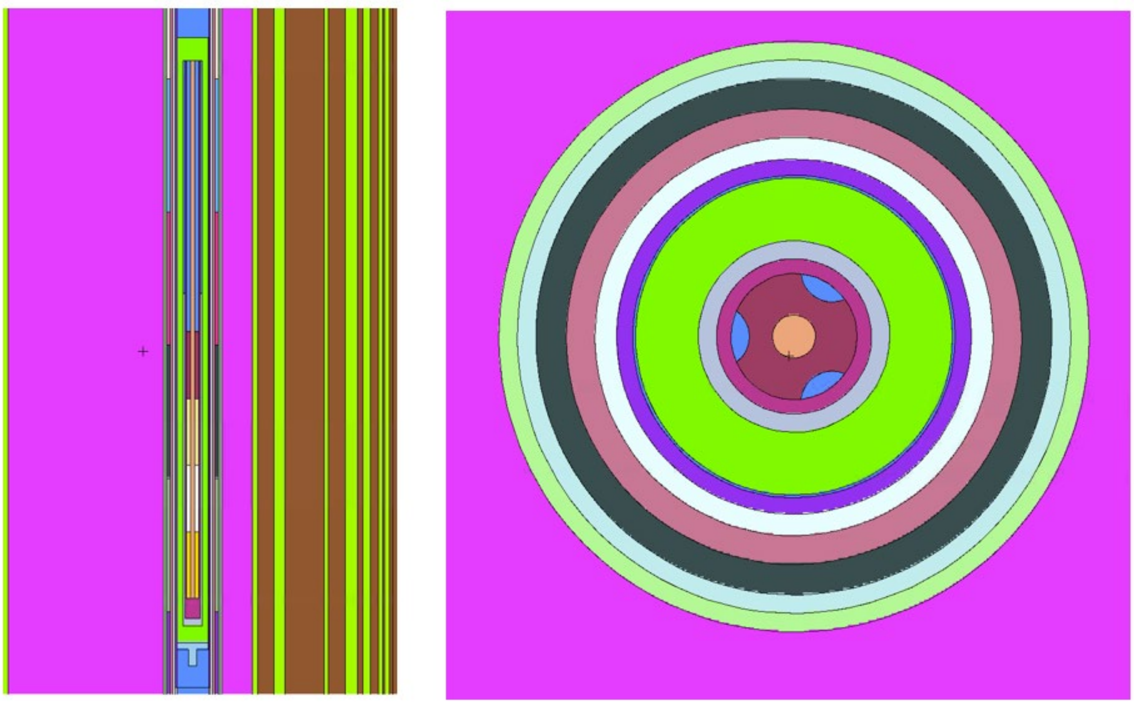

Figure 11: Shows an axial cross section (left) and top-down cross section (right) view of the IMPACT slotted fuel outer capsule as modeled in MCNP.

Neutronic calculations were performed for three cycles, each of 60 effective full-power days (EFPDs) in the ATR B3 position, with the experiment installed in a cadmium-shrouded basket. Prolonged ATR cycles of 65 EFPDs are considered when analyzing experiment fuel and cadmium burnup. Because of different axial positions in the core, a sensitivity analysis was performed to determine the enrichment required for each fuel specimen to maintain the desired BOI LHGRs. Enrichments of each fuel specimen are reported in Table 2, and Table 3 provides the resulting BOI LHGR for each axial section of fuel specimen at the identified enrichments. These sections are averaged to provide each specimen's LHGR. The reported averaged LHGRs fall within the 325 ± 50 W/cm requirement listed in Table 1. The outer diameter power for each specimen was calculated and compared to average power across the specimen. Each specimen showed less than 1.5× average radial power in the outer diameter power.

Table 2: Lists the final experiment fuel inner diameter (ID) and outer diameter (OD) and enrichments for each capsule.

Capsule Position	Fuel	Enrichment [wt% U235]	Fuel OD [cm]	Fuel ID [cm]	Fuel Length [cm]
1 (Bottom)	Sodium-bonded	54	0.437	0.163	10.160
2	Annular	47	0.475	0.246	10.160
3	Slotted[a]	59	0.475	0.163	10.160
4 (Top)	Non-fueled	-	-	-	-
[a] The slotted fuel specimen has three hemispherical grooves that are 120º apart.					

Table 3: Lists modeled experiment fuel heat generation rate (HGR) and LHGRs for each rodlet.

Fuel	Section	Scaled Core Power [MW]	HGR [W/g]	LHGR [W/cm]	Average LHGR [W/cm]
Sodium-bonded	1	104.6	149.54	309.15	322.11
	2	104.6	152.35	314.95	
	3	104.6	158.03	326.69	
	4	104.6	163.33	337.65	
Annular	1	104.6	158.79	325.96	322.26
	2	104.6	155.33	318.86	
	3	104.6	155.99	320.23	
	4	104.6	157.82	323.98	
Slotted	1	104.6	165.22	338.17	321.68
	2	104.6	160.14	327.78	
	3	104.6	154.19	315.60	
	4	104.6	149.10	305.17	

Fuel burnup was calculated at the end of each cycle and is reported in Table 4. Fuel specimens in the IMPACT experiment are expected to reach a total burnup of 15% by the end of the third cycle, doubling the percentage of required burnup for the experiment objectives. Cadmium burnup is calculated and limited to approximately 120 EFPDs (consistent with historical usage) for thermal neutron shielding. Therefore, the experiment was designed to replace the cadmium-shrouded basket after the first ATR cycle, and a second cadmium shroud is installed for the remaining two cycles of irradiation. The total fission gas (primarily xenon and krypton isotopes) produced in the rodlet at these burnups was calculated to inform on gaseous pressures inside of the rodlet and inform structural analysis for various operational conditions. No fuel fission gas retention was considered, and analysis assumes 100% fission gas release in rodlet pressure calculations for conservatism.

Table 4: Lists modeled experiment fuel burnup at the end of each ATR cycle (60 EPFDs).

Fuel	End of 1st Cycle [at%]	End of 2nd Cycle [at%]	End of 3rd Cycle [at%]
Sodium-bonded	4.94	9.57	14.4
Annular	4.99	9.65	14.5
Slotted	4.98	9.65	14.5

4.2 THERMAL ANALYSIS

Neutronics LHGRs from both fuel and surrounding structural materials were fed into the thermal ABAQUS model of the experiment. The purpose of the thermal model was to assess thermal expansion within the capsule, the gas gap and gas mixture between the inner and outer capsules, and the resulting temperatures within the experiment during operation. Pressures resulting from operational temperatures were also calculated as part of the thermal modeling. The temperatures of the capsules containments and the peak internal cladding temperature (PICT) are controlled by the gas gap and gas composition between in the inner capsule and the outer capsule. As stated previously, a pure He atmosphere was chosen for this experiment as the gas gap composition, and the adjustment of conductivity was achieved via the machining of the outer diameter of the inner capsule and resulting gas gap. This gap changes as a function of the temperature of the inner capsule due to thermal expansion and thus must be evaluated for a range of temperatures.

Both 2D and 3D ABAQUS finite element models were generated to evaluate the thermal conditions in the IMPACT experiment. The 2D model was used to simulate gap closure due to thermal expansion of the outer and inner-capsule gap. Temperatures were higher than desirable when thermal expansion was neglected in the 3D model. Therefore, the 2D model was used to simulate the gap closure which was then applied to the 3D model to produce more accurate temperature results; ultimately the temperatures in the experiment were evaluated with the "hot gap" due to expansion. To accomplish this, the thermally expanded gap was measured in the 2D model between the inner capsule and outer capsule for Capsules 1–3. See Figure 13 for measurement locations of the gap in the 2D model. The resulting gap was measured and then simulated in the 3D model using the built-in interaction properties in ABAQUS. Based on 2D analysis iterations the nominal machined gas gap for the experiment was 0.10mm with a pure He atmosphere pressurized to 1.21MPa, and the "hot gap" was approximately 0.05 mm for each capsule to achieve desired temperatures.

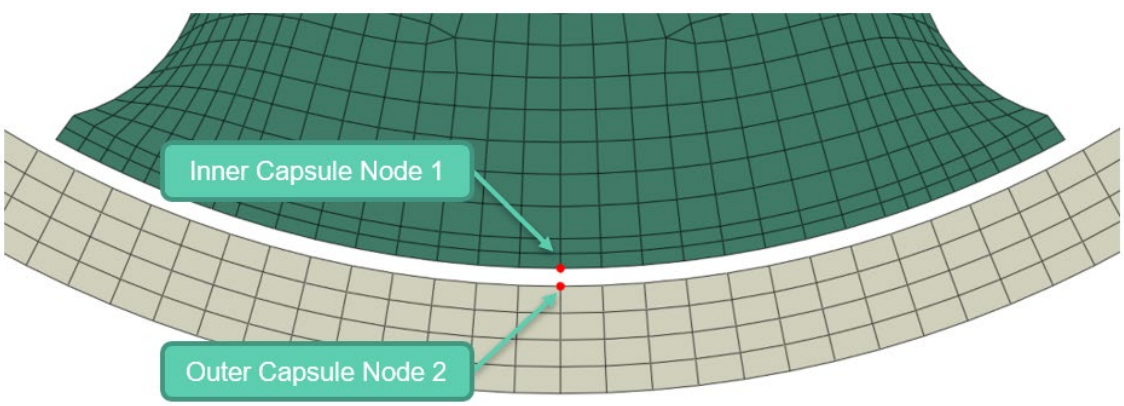

Figure 12: Shows a top-down cross section view of the gas gap between in the inner and outer capsule.

Desired PICT was designed to be between 500 and 650°C for all rodlets. Burnup in the fuel was considered during the duration of the experiment as fuel burnup will decrease heating and PICT as irradiation days increase. Thus, the highest temperatures experienced by experiment components during normal operation will occur at BOI temperatures shown below in Figure 14. Instrumentation was included in the programmatic case due to the high temperatures of the inner capsule. This method accounts for the best possible prediction of inner and outer-capsule temperatures for use in structural analysis.

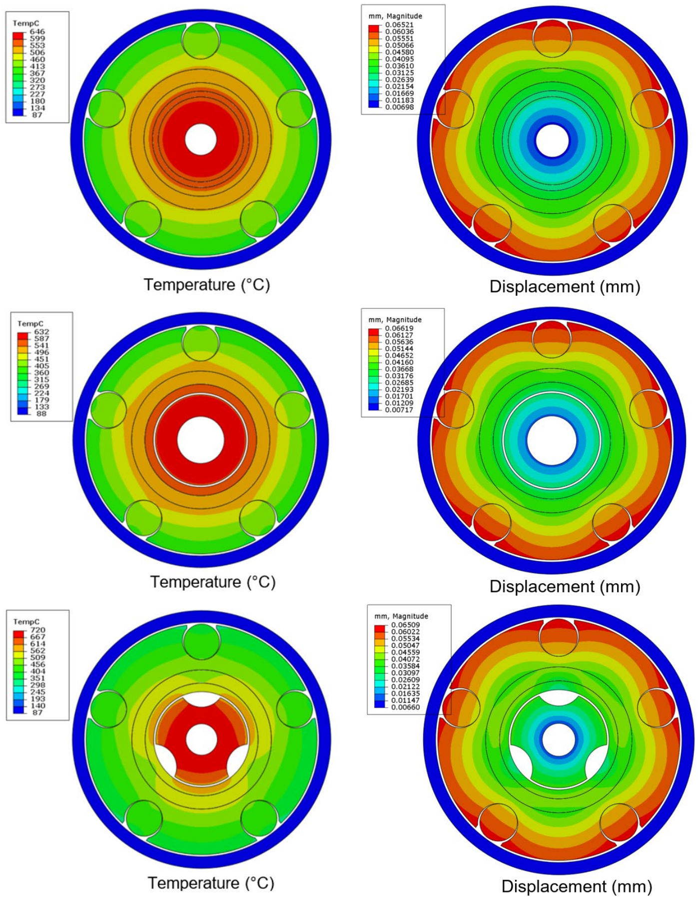

Figure 13: Shows top-down cross-section views of the IMPACT capsules with resulting temperatures (left) (°C) and displacement due to thermal expansion (right) in mm.

The ABAQUS 3D models shown in Figure 14 were generated using DC3D8 (an eight-node linear heat transfer brick element), DC3D4 (a four-node linear heat transfer tetrahedron element), and DCC3D8 elements (an eight-node convection/diffusion brick element). Iterations were required to set water temperatures accurately in the 2D model film condition based on results from the 3D model. The peak 3D water temperature was used for simplicity and was then included in the film condition applied to the outer-capsule surface of the 2D model. A half cross-section model was used to reduce the overall number of mesh elements while still accounting for geometry that could not be considered for an axisymmetric model. Model geometry for IMPACT was unique, but it can still be considered symmetric along the cut plane as seen in Figure 15. The model includes the four IMPACT experiment capsules, the outer capsule, the experiment basket, and test stop assembly, a 0.64cm thick section of beryllium, and an inner and outer water channel. Thermal 3D models were used for safety analysis of experiment operation and resulting temperatures and pressures were input into structural analysis.

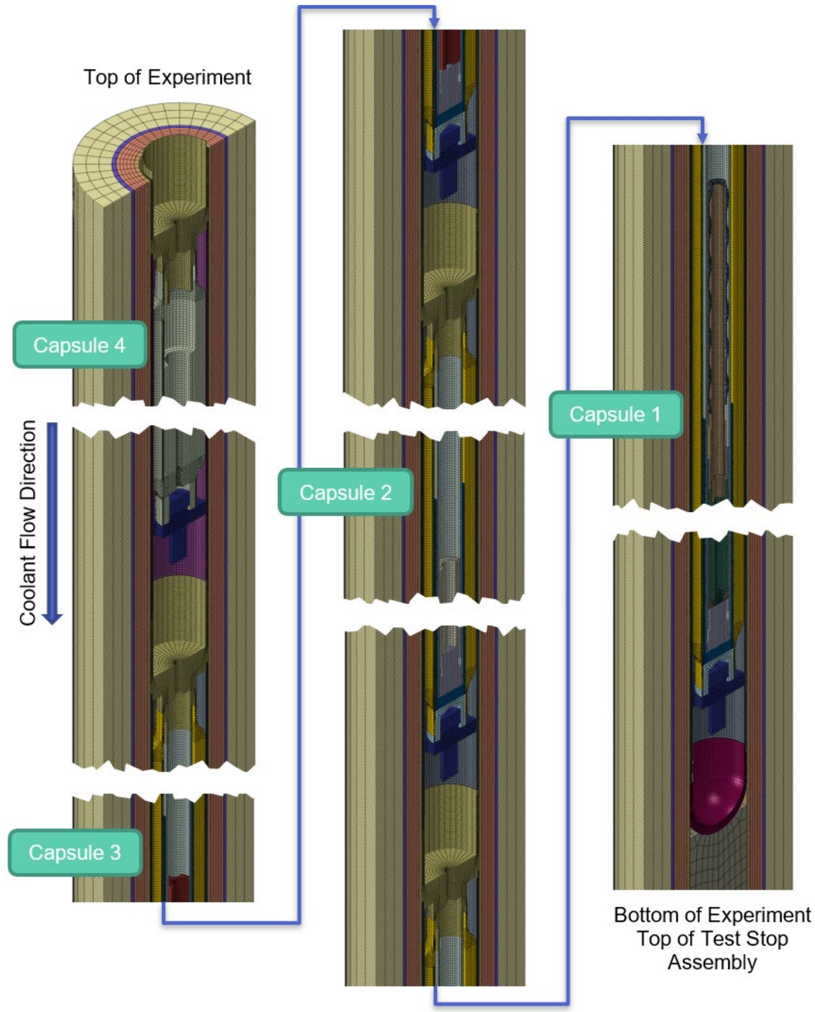

Figure 14: Shows axial cross section views of the IMPACT capsules in 3D modeled in ABAQUS.

Figure 16 and Table 6 show final temperatures for each capsule during normal operation. Results are reported here in °F for input into ASME BPVC structural analysis. Note that the outer capsule for each capsule is reported as one maximum temperature of 133°C. Temperatures within Capsule 3 components show the highest PICT of 602°C and an inner capsule temperature of 529°C. Flow coastdown and RIA temperatures were calculated with a conservative east lobe power of 28 MW (indicated) plus additional safety factors: 8.5% factor for instrument uncertainty and an additional 18% multiplier for ATR outer shim control cylinder rotation. Water temperatures and corresponding surface heat fluxes were used to calculate Flow Instability Ratio (FIR) and Departure from Nucleate Boiling Ratio (DNBR), where FIR and DNBR were shown to be greater than 2. During these events the PICT of rodlet reaches 850–890°C and the inner capsule peak temperature reaches 740–750°C in Capsule 3. The temperatures in this section were considered conservative for structural analysis assuming rodlet or inner capsule failure. Results show low outer-capsule temperatures, low water channel temperatures, and low outer-capsule surface heat fluxes, which are acceptable for operation during these events.

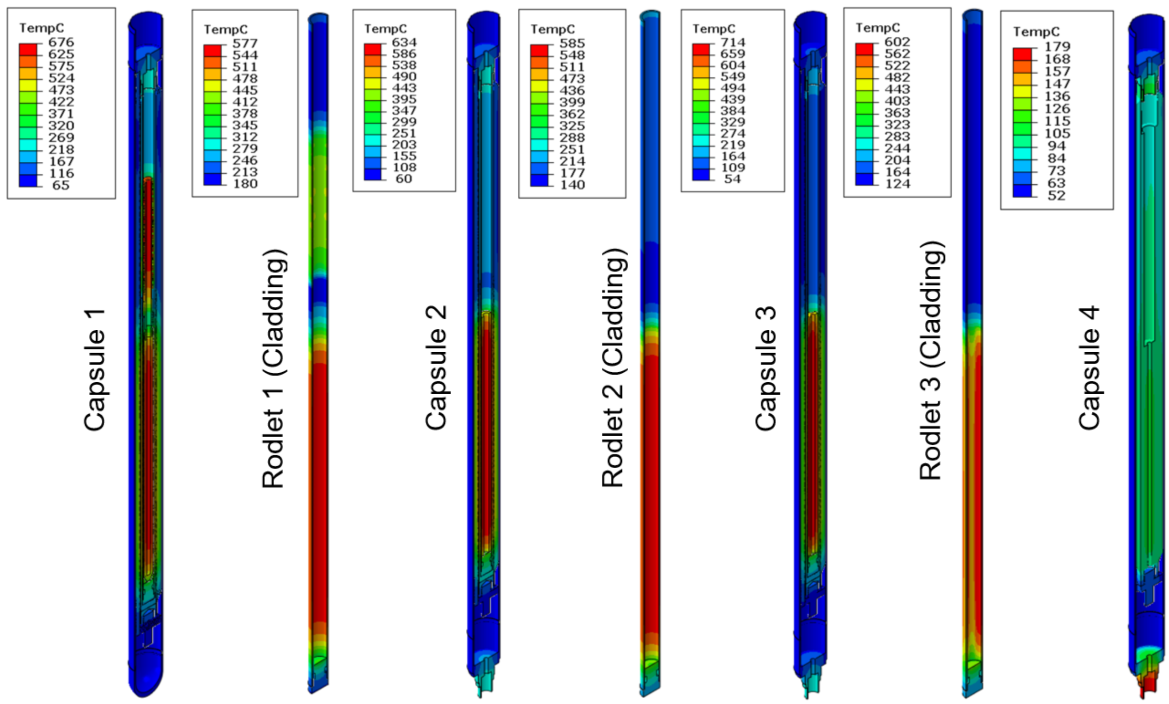

Figure 15: Shows axial cross section views of the IMPACT capsules and rodlets with resulting temperatures (°C).

Table 5: Lists resulting modeled temperatures (°C) for each IMPACT capsule components and other assembly components.

	ABAQUS Component	Material		
			°C	°C
	Inner Capsule 4	SS316L	106	1370
Capsule 3	Inner Capsule 3	SS316L	529	1370
	Rodlet 3	SS316L	602	1370
	Fuel 3	U10Zr	713	1248
Capsule 2	Inner Capsule 2	SS316L	530	1370
	Rodlet 2	SS316L	585	1370
	Fuel 2	U10Zr	634	1248
Capsule 1	Inner Capsule 1	SS316L	523	1370
	Rodlet 1	SS316L	577	1370
	Fuel 1	U10Zr	650	1248
	Splash Guard	U10Zr (Depleted)	676	1248
	Wave Conductor	Inconel 600	655	1354
Other	Outer Capsule	SS316L	133	1370
	Basket Sleeve	Aluminum 6061	69	582
	Cadmium Filter	Cadmium	69	321
	Test Stop	Nitronic 60	88	1450
		SS304		1400

4.3 STRUCTURAL ANALYSIS

Structural analysis was performed to assess the experiment integrity for design and during operation. Analysis activities include the evaluation of structural integrity of THCP-MkII seal hardware, experiment leadout components, experiment inner and outer capsules, and fuel rodlets. THCP-MkII hardware includes the seal plug, seal sleeve, seal plug flange and washer, closure ring, and associated bolting hardware, shown in Figure 4, above. As part of the ATR reactor pressure vessel (RPV) seal, THCP-MkII hardware uses ASME BPVC Section III, Division 1, Class 1, subarticle NB-3300, "Vessel Design" [3], acceptance criteria for structural evaluation. Pressures on THCP-MkII seal hardware are from ATR primary coolant at a design temperature of 51°C and design pressure of 2.45 MPa. The ATR RPV coolant applies a load of 2.69 MPa for normal operation and 3.23 MPa during an off-normal operational event such as flow coastdown.

Outer capsules and leadout components use ASME BPVC Section III Subsection ND, Class 2 and Class 3, subarticle NCD-3300, "Vessel Design" [2] acceptance criteria for evaluation. While inner capsules and rodlets were only considered secondary containment, they were also evaluated to the same acceptance criteria. During normal operations, rodlet pressures at temperature meet most of the requirements of ASME Section III, Class 3 [2]. As can be seen from Table 6, the temperatures for these components are over 426°C which is beyond the published material temperatures for ASME BPVC Section III Class 3 components. Therefore, ASME BPVC Section III, Division 5, "High Temperature Reactors" was used for inner-capsule evaluation. Specifically, Subsection HC, Class B Metallic Pressure Boundary Components [7] was used. Because rodlet material temperatures during off-normal operational events are beyond the temperatures listed in ASME Section II [8], no evaluation was performed for the rodlets in these conditions. Pressure in the inner capsule was calculated to be less than 0.21MPa during normal operating conditions. With the production of gaseous fission products within the rodlet, the pressures increase as a function of the burnup of the fuel, and for conservatism it was assumed that all fission gases are released into the rodlet plenum. Rodlet pressures were calculated to be 4.51 MPa for Rodlet 1 and approximately 3.10 MPa for Rodlet 2 and Rodlet 3. Ultimately, because the outer capsule was credited as the primary pressure boundary, it must meet all requirements for ASME Section III, Class 3 during normal operation and off-normal operation events. Initial conditions of the leadout components and outer capsule are an internal design pressure of 1.21 MPa, and the ATR coolant temperature of 51°C. During all experiment operating conditions, the pressure within the leadout components and outer capsule was 1.35 MPa.

An additional off-normal ASME BPVC Section III, Service Level D condition was considered for the retention of pressure in the outer capsule. An accident scenario was postulated regarding water ingress through a pin-hole leak in the outer capsule and the failure of the inner capsule, causing a sodium-water chemical interaction within the inner capsule. As a result of the interaction, moles of hydrogen gas are produced and fill the cavities of the inner and outer capsule. It was assumed in this scenario that the original leak from the outer capsule is closed, and that pressure is retained during this event. The total moles of hydrogen and sodium hydroxide were calculated based on the available reactants in the inner volume of the inner capsules and the ideal gas law was used to calculate the pressure in the outer capsule (including free volume in the leadout components). Considering gas compressibility, the pressure in the outer capsule was calculated to be 9.74 MPa.

Per ASME BPVC Section III, Division 1, Subsection NB, Class 1, the maximum Tresca stress from the finite-element model was compared with the allowable stress for P_m [3].

$$DC = \frac{(P_m \; or \; P_L) + P_b + F}{S_m} < 1.0 \tag{1}$$

where P_m is the general membrane stress, P_L is the local membrane stress, P_b is the bending stress and F is the peak stress. Typically, the largest of P_m versus P_L is used in the structural analysis. The numerator, $(P_m \; or \; P_L) + P_b + F$, is the maximum Tresca stress, and $Demand - to - Capacity \; (DC)$ ratio is the ratio between the Tresca stress and the allowable and must be less than 1.0 for acceptance; this was conservative, as the highest stress was being compared with the lowest allowable stress. Additional evaluations were performed per the ASME BPVC such as the inclusion of any secondary stresses on the system (where Tresca would be considered the primary stresses). Secondary stresses in the components were assumed to be thermal stresses in this analysis, and were added to the Tresca stress and compared to the allowable per Equation 2 [3].

$$DC = \frac{P + Q}{S_m} < 1.0 \tag{2}$$

An additional check was performed for thermal ratcheting, which includes a cyclic consideration to thermal stresses in the system. The stress allowable for the various components were compared to these stresses modeled and calculated using a finite element analysis software, ABAQUS. Because the loading cycles envisioned for the experiment are below 10 (three ATR cycles planned) the experiment was not analyzed for fatigue.

The IMPACT components have one plane of symmetry so only one-half of the parts were modeled as shown in Figure 17 and Figure 18. Mesh elements for the THCP-MkII sealing components and outer-capsule components were eight-node linear bricks with incompatible modes (ABAQUS C3D8I element type). The closure ring contains ten-node quadratic tetrahedron elements (ABAQUS C3D10 element type) as the geometry was too intricate to mesh with brick elements. The inner capsule contains some ten-node quadratic tetrahedron elements (ABAQUS C3D10 element type) as the geometry was too intricate to mesh with brick elements. Surfaces between components were modeled with "hard" contact. Welds in the analysis were assumed to be full-penetration welds with the same stiffness and strength as the base material. Weld joint efficiency is defined as 0.45 for a Type 6 weld that is neither fully radiographed nor spot radiographed during assembly per ASME BPVC Section III. For tangential behavior, the penalty formulation was used with a friction coefficient of 0.3. Loads on the THCP sealing components are both reactor coolant pressure and bolt preloads. Bolts and other hardware were also analyzed in ABAQUS. Loads on outer capsules are reactor coolant pressure and internal pressures as a result of all operating conditions. While leadout components were analyzed separately from the outer capsules, due to the drastically thicker wall of the leadout components, the resulting stresses in these components were bounded by the outer capsule analysis. The component mesh and ABAQUS stress analysis can be seen in Figure 17 and Figure 18. Results of the ASME BPVC analysis are recorded in Table 7 and Table 8. Per Table 7, below, the evaluation of the THCP-MkII sealing components meets ASME BPVC Section III, Class 1 requirements and is acceptable for the experiment reactor operation. Table 8 shows that the outer capsule and leadout components meet ASME BPVC Section II Class 3 requirements and is also acceptable for experiment reactor operation.

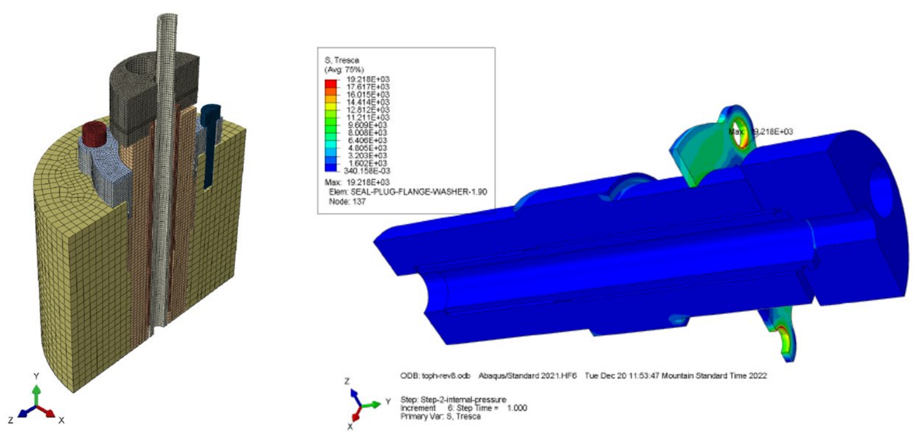

Figure 16: Shows axial cross section views of the IMPACT THCP-MkII sealing hardware ABAQUS model (left), and the ABAQUS Tresca stress results (right).

Table 6: Lists the ASME Section III, Class 1 THCP sealing hardware analysis results for the DC ratio (must be <1.0).

Condition	Stress Category	DC Ratio
Design	P_m	0.134

	Triaxial	0.045
Level A	P + Q	0.194
	Thermal Stress Ratcheting	0.027
	Cyclic Operation	N/A
Level C	P_m	0.114

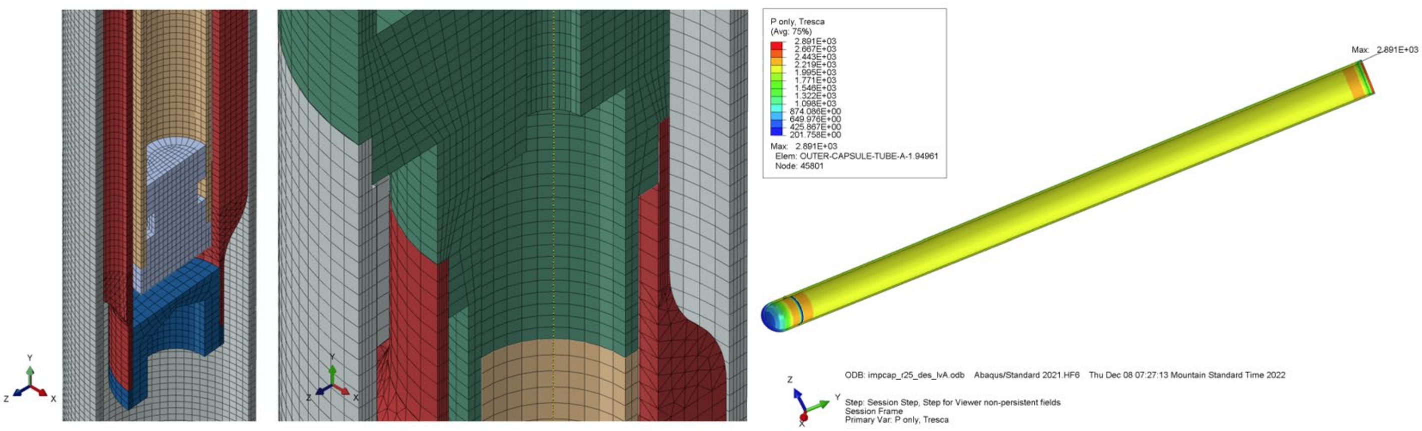

Figure 17: Shows axial cross section views of the IMPACT capsule ABAQUS model (left), and the ABAQUS Tresca stress results on the outer capsule (right).

Table 7: Lists the ASME Section III Class 3 outer-capsule analysis results for the DC ratio (must be <1.0).

Condition	Stress Category	DC Ratio
Design	P_m	0.111
Level A	P + Q	0.647
	Thermal Stress Ratcheting	0.830
	Cyclic Operation	N/A
Level C-1 Flow Coastdown	P_m	0.078
Level C-2 RIA	P_m	0.077
Level D Sodium-Water Interaction	P_m	0.301

5. FUTURE WORK

The IMPACT experiment is moving forward with the completion of the final design. Flow-induced vibration analysis will be performed for the leadout section of the experiment to ensure that no resonant frequencies are observed during reactor operation. Neutronics sensitivity studies will be completed for additional ATR EFPDs per cycle to ensure that additional fuel or cadmium burnup does not drastically affect the heating rates in the experiment. This analysis encompasses all scenarios where sections of the experiment may be uncovered by water (where the primary modes of heat transfer are natural convection and radiation). Additional out-of-pile design activities are required, including tooling, supporting installation hardware, and hardware testing apparatuses. Fabrication and assembly are underway for the IMPACT experiment, including weld and braze development activities for qualification. The thermal conductivity sensor fabrication is underway and calibration facilities have been used for sensor qualification. Brazing of the sensor into the capsule bulkhead has been successfully prototyped. Digital twin models are being developed for sensor operation in-pile.

6. CONCLUSION

The IMPACT experiment will be the first in a series of instrumented capsule experiments in ATR to irradiate various advanced nuclear fuel specimens and materials with embedded thermal conductivity probes. This design will accelerate irradiation experiment data collection by utilizing novel in situ instrumentation, eliminating the need for a considerable number of drop-in capsules with discrete burnup or displacements per atom (DPA) targets. Future experiments employing this new capability may be designed to explore different instrumentation or gas lines into the experiment. Additionally, this experiment design bridges the gap between the cost of drop-in experiments and typical leadout experiments at ATR, providing a wider range of experimental options for customers. As the first experiment of this kind, IMPACT will provide data that describe the thermal properties evolution of three metallic fuel designs to inform fuel performance models and optimize reactor designs using uranium 10 wt% zirconium (U10Zr). The current work describes the final design of the IMPACT experiment and supporting analysis performed to ensure that the functional requirements are met. Experiment design was executed, including neutronics analysis, thermal hydraulic analysis, structural analysis, and the final mechanical design of the experiment hardware. Analysis confirmed that the IMPACT experiment is sufficient for installation and operation in ATR under all operational conditions considered. Design process and analysis reported is envisioned for future experiments similar to IMPACT for additional fuel and structural materials irradiation experiments. Fuels or materials intended for irradiation at lower temperatures using the IMPACT design may be bounded by the current analysis for U10Zr fuels at 600°C. Custom rodlet and inner-capsule designs are possible for future instrumented capsule designs, and analysis outlined in the current work will be repeated for those geometries and materials. More instrumented capsule designs of this kind may be investigated for other ATR irradiation positions, such as the medium-I positions.

ACKNOWLEDGEMENTS

This research work was prepared for the U.S. Department of Energy through the INL LDRD program, grant number 22A1059-134FP, under the DOE Idaho Operations Office. It also made use of INL's high-performance computing resources. Contract No. DE-AC07-05ID14517.

REFERENCES

[1] L. C. W. T.H. Bauer, G.L. Hofman, "97/01950 Metallic fast reactor fuels," *Fuel Energy Abstr.*, vol. 38, no. 3, p. 158, 1997, doi: 10.1016/s0140-6701(97)87870-8.

[2] ASME, "ASME BPVC Section III Division 1, Subsection ND," *ASME Boil. Press. Vessel Code,* 2023.

[3] ASME, "ASME BPVC Section III Division 1, Subsection NB," *ASME Boil. Press. Vessel Code*, 2023.

[4] C. Hollar, A. Fleming, K. Davis, R. Budwig, C. Jensen, and D. Estrada, "A parametric study for in-pile use of the thermal conductivity needle probe using a transient, multilayered analytical model," *Int. J. Therm. Sci.*, vol. 145, no. July, p. 106028, 2019, doi: 10.1016/j.ijthermalsci.2019.106028.

[5] K. Wada, A. Fleming, J. Eixenberger, B. J. Jaques, and D. Estrada, "Transient multilayer analytical model of a line heat source probe for in-pile thermal conductivity measurements," *Int. J. Therm. Sci.*, vol. 188, no. January, p. 108241, 2023, doi: 10.1016/j.ijthermalsci.2023.108241.

[6] ASME, "ASME BPVC Section IX," American Society of Mechanical Engineers, 2023.

[7] ASME, "ASME BPVC Section III Division 5, Subsection HC," American Society of Mechanical Engineers, 2023.

[8] ASME, "ASME BPVC Section II," American Society of Mechanical Engineers, 2023.